ARTICLE

BIOTECHNOLOGY and BIOENGINEERING

A Stochastic Model for Predicting Dextrose Equivalent and Saccharide Composition During Hydrolysis of Starch by α-Amylase

Tamara Besselink, Tim Baks, Anja E.M. Janssen, Remko M. Boom

Food and Bioprocess Engineering Group, Wageningen University and Research Centre, P.O. Box 8129, 6700 EV, Wageningen, the Netherlands; telephone: +31-317-48-37-70; fax: +31-317-48-22-37; e-mail: tim.baks@wur.nl

Received 24 July 2007; revision received 20 November 2007; accepted 18 December 2007

Published online 30 January 2008 in Wiley InterScience (www.interscience.wiley.com). DOI 10.1002/bit.21799

ABSTRACT: A stochastic model was developed that was used to describe the formation and breakdown of all saccharides involved during α-amylolytic starch hydrolysis in time. This model is based on the subsite maps found in literature for *Bacillus amyloliquefaciens* α-amylase (BAA) and *Bacillus licheniformis* α-amylase (BLA). Carbohydrate substrates were modeled in a relatively simple two-dimensional matrix. The predicted weight fractions of carbohydrates ranging from glucose to heptasaccharides and the predicted dextrose equivalent showed the same trend and order of magnitude as the corresponding experimental values. However, the absolute values were not the same. In case a well-defined substrate such as maltohexaose was used, comparable differences between the experimental and simulated data were observed indicating that the substrate model for starch does not cause these deviations. After changing the subsite map of BLA and the ratio between the time required for a productive and a non-productive attack for BAA, a better agreement between the model data and the experimental data was observed. Although the model input should be improved for more accurate predictions, the model can already be used to gain knowledge about the concentrations of all carbohydrates during hydrolysis with an α-amylase. In addition, this model also seems to be applicable to other depolymerase-based systems.

Biotechnol. Bioeng. 2008;100: 684–697.

KEYWORDS: α-amylase; starch hydrolysis; modeling; stochastic model; subsite mapping; amylopectin structure

Introduction

The hydrolysis of starch by amylolytic enzymes is one of the most important enzymatic processes on industrial scale. Starch can be completely hydrolyzed to produce glucose syrups or, alternatively, it can be partly hydrolyzed to yield maltodextrins. Many models have been developed to predict the concentrations of the different hydrolysis products and to optimize the hydrolysis process. These models can be roughly divided into two groups.

The first group of models is based on continuous (differential) equations (Brandam et al., 2003; Komolprasert and Ofoly, 1991; Kusunoki et al., 1982; Park and Rollings, 1994; Rodríguez et al., 2006a; Rollings and Thompson, 1984) or empirical relations (Paolucci-Jeanjean et al., 2000) for the description of the enzymatic starch hydrolysis. Most of these models only predict the breakdown and/or formation of a limited number of carbohydrates, because each prediction requires a differential equation or empirical relation. The number of predictions that can be made is therefore limited to computational power. In addition, the parameters in the equations have to be obtained by fitting model output to the experimental data. This type of kinetic modeling is therefore also limited to data that can be obtained with measurements and it is only valid for specific experimental conditions.

The other group of models simulates the hydrolysis process by translating each hydrolysis reaction into a discrete event (Marchal et al., 2003; Nakatani, 1996; Wojciechowski et al., 2001). During each event, a carbohydrate is chosen randomly to form a complex with the enzyme. Whether a bond in the carbohydrate is hydrolyzed, depends on enzyme characteristics. It is important that the substrate and the enzyme specificities are clearly defined in order to make accurate predictions of product profiles. This stochastic method can be used to describe the formation and breakdown of all carbohydrates without determination of numerous parameters and evaluation of large numbers of (dependent) equations. Contrary to the output of the first group of kinetic models, the output of the second group can vary even though the input parameters are kept the same, which resembles real-life hydrolysis.

Correspondence to: T. Baks

An example of the models belonging to the second group is the stochastic model developed by Wojciechowski et al. (2001). They used the Monte Carlo method to describe the products formed during multi-enzymatic starch hydrolysis in time. They proposed that each enzyme has a certain reaction time and specificity for hydrolysis (e.g., hydrolysis near a branch point is not possible). Differences in substrate affinities were not taken into account. Furthermore, the authors did not focus on the amylopectin and amylose model structure (e.g., percentage of branched glucose units and chain length distribution). The validity of their model was evaluated by comparing the reducing power of the reaction mixture predicted by the model with the experimental values at various points in time.

Another model belonging to the second group was developed by Marchal et al. (2001, 2003). These authors proposed a method to model amylopectin and the subsequent α-amylolysis by *Bacillus amyloliquefaciens* α-amylase (BAA). They used stochastic Monte Carlo simulation in combination with the subsite theory (Allen and Thoma, 1976a,b; MacGregor and MacGregor, 1985) to describe the carbohydrate composition as a function of the dextrose equivalent (DE). The data obtained with the model simulations were compared to experimental data for the formation and breakdown of carbohydrates up to a degree of polymerization (DP) of 10. With the model of Marchal et al. (2003), it is possible to predict the carbohydrate composition at a certain DE. However, it was not possible to predict the concentration of hydrolysis products in time.

Although several models have thus been developed to describe enzymatic starch hydrolysis, a kinetic model that takes the structure and composition of starch into account and that predicts the concentration of all carbohydrates in time has not been developed yet.

The aim of this article was to develop a stochastic model to predict the formation and breakdown of all carbohydrates involved in the amylolytic hydrolysis of amylopectin and amylose in time with a minimum number of experiments. The subsite maps of *Bacillus licheniformis* α-amylase (BLA) from Kandra et al. (2002) and of BAA from Allen and Thoma (1976b) were used as input for this model. In addition, a method to model the structure of starch was developed. This starch model was used as input for the kinetic model. Since the subsite maps used for our model were experimentally determined using small linear carbohydrates [DP up to 12 for BAA, Allen and Thoma (1976b); and up to 10 for BLA, Kandra et al. (2002)], we also wanted to investigate whether these subsite maps could be used to describe the breakdown of large carbohydrates in time. The data calculated with the model are compared with experimental data for wheat starch hydrolysis by both BAA and BLA.

Modeling

Modeling of Starch

Marchal et al. (2001) proposed that the structure of starch can be captured using a two-dimensional array in which letters were used to describe the glucose units in amylopectin. Wojciechowski et al. (2001) used two numbers to describe each glucose unit, which makes the data set for the description of amylopectin larger than necessary.

In our model, we have used numbers to distinguish five different types of glucose units in amylopectin and amylose. A reducing end is given the number 1, the number 3 is used for the non-reducing end. The number 2 stands for a glucose unit in a linear α-1,4-linked chain. A branched monomer is denoted with a negative number. The same number but positive points to the row in which the branch is located. This branch starts with the number 4 to distinguish it from a reducing end. An example of the amylopectin model structure and the representative matrix is given in Figure 1.

The model described in this article takes into account several structural aspects of starch. First, the model includes

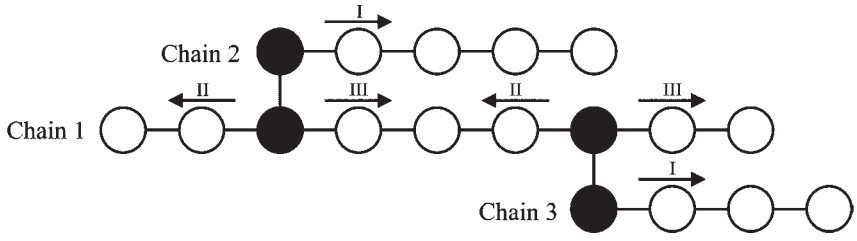

Chain	Glucose units								
1	1	2	-2	2	2	2	-3	2	3
2	4	2	2	2	3	0	0	0	0
3	4	2	2	3	0	0	0	0	0

Figure 1. Example of amylopectin model structure and matrix. The carbohydrate is drawn with the reducing end to the left and the non-reducing ends to the right. Filled circles indicate α-1,6-linked glucose units. The arrows with Roman numbers I, II, and III indicate the type of inhibition from α-1,6-linked glucose units. See text for more details on nomenclature and inhibition.

the fact that starch consists of approximately 25 w/w% amylose and 75 w/w% amylopectin. Second, amylose is an almost linear polymer with an average molecular weight of 10^5–10^6 g mol^{-1} built up from α-1,4-linked glucose units. Third, the much larger amylopectin (molecular weight of 10^7–10^9 g mol^{-1}) has a highly branched structure, because about 5% of the glucose units in amylopectin are α-1,6-linked (Ellis et al., 1998). Finally, the modeled amylopectin has to comply with four constraints with respect to glycosidic α-1,6-linkages, as stated by Thompson (2000): amylopectin does not contain linear α-1,6-linked regions; α-1,4-linkages are more abundant than α-1,6-linkages; glucose units cannot have more than one side chain; and branch points are always at least one glucose unit apart. An additional assumption was that branching can only occur when the glucose unit is at least 1 glucose unit apart from a reducing or non-reducing end.

To model starch, we started with a model for amylopectin. At the start, the largest chain in amylopectin is placed on the first row of the substrate array. A random number generator was used to generate a number between 0 and 1 for the first glucose unit capable of branching. If the number was smaller than the chance of branching, a side chain was attached to this glucose unit. If branching did not occur, the program proceeded to the next glucose unit. The restrictions stated by Thompson (2000) were taken into account during this procedure. It was assumed that the probability that a branch chain of a certain length is implemented in the molecule is proportional to its molar fraction in amylopectin.

If a branch chain was attached to the glucose unit, a new row was added to the bottom of the array. The number representing the glucose unit changed into a negative number that directed to index of the row in the matrix that contained the description of the newly implemented chain. This procedure was continued until the desired size of amylopectin was reached. It was possible that no more branch points were created, even though the desired size was not yet reached. In that case, the last row in the array was forced to branch. As a result, the actual fraction of branched glucose units could be slightly higher than desired.

Subsequently, amylose chains were added to the substrate matrix until the desired fraction of amylose was obtained. This fraction could vary depending on the size of the chains implemented. The starch model described here was used as input for the modeling of enzymatic starch hydrolysis.

Modeling of Enzymatic Starch Hydrolysis

The subsite theory for depolymerizing enzymes (Allen and Thoma, 1976a,b; MacGregor and MacGregor, 1985; Torgerson et al., 1979a,b) was used as the basis for the hydrolysis model. According to this theory, the enzyme is composed of several subsites to which the monomers (in this case glucose units) can bind. Each subsite can increase or decrease the free energy of the enzyme–substrate complex. The following reaction scheme is used to describe the hydrolysis of substrate S_n with DP n by the enzyme E into products P_{n-m} and P_m (the use of water is not shown):

$$E + S_n \underset{k_{-1,r,n}}{\overset{k_{+1,r,n}}{\rightleftharpoons}} ES_{r,n} \xrightarrow{k_{+2,r,n}} E + P_{n-m} + P_m \qquad (1)$$

where r refers to the position of the reducing end of the saccharide in the subsite map. The subsite theory assumes that $k_{+2,r,n} \ll k_{-1,r,n}$, which implies that $K_{r,n}$ (the association constant for the enzyme–substrate complex) is equal to $k_{+1,r,n}/k_{-1,r,n}$. $K_{r,n}$ can be calculated from the binding energies of the occupied subsites (Allen and Thoma, 1976a; MacGregor and MacGregor, 1985; Marchal et al., 2003; Torgerson et al., 1979) with the following equation:

$$-RT\ln(K_{r,n}) = \sum_{i=r-n+1}^{r} \Delta G_i + \Delta G_{\mathrm{mix}} \qquad (2)$$

where R is the gas constant, T the absolute temperature in Kelvin, ΔG_i the binding energy of subsite i and $\Delta G_{\mathrm{mix}} = 8.4T\ln(55.5)$ kcal mol^{-1} for bimolecular processes (Gurney, 1953 by Marchal et al., 2003). Note that subsite r might be a virtual subsite with zero binding energy, because it is located outside the subsite map.

If a substrate forms a complex with the enzyme, the complex is only productive when the substrate occupies the subsites to the left and right of the location of hydrolysis (subsites −1 and +1 according to the nomenclature defined by Davies et al., 1997). If all enzymes in the reaction mixture are saturated with substrate, the rate of hydrolysis is limited by $k_{+2,r,n}$. The value of $k_{+2,r,n}$ may be assumed constant for all substrate sizes and binding modes, or it may be varied. To enhance the agreement between model data and experimental data, some subsite maps use an acceleration factor proportional to the number of subsites occupied (x) using the following relation:

$$k_{+2,r,n} = k_{+2}\exp\left(\frac{x\Delta G_{\mathrm{a}}}{RT}\right) \qquad (3)$$

where ΔG_{a} is the acceleration factor of the subsite map (Allen and Thoma, 1976a; Torgerson et al., 1979). For more details on the subsite theory, we refer to literature (Allen and Thoma, 1976a,b; MacGregor and MacGregor, 1985; Torgerson et al., 1979).

To simulate the hydrolysis process, a random number was generated to select an element in the substrate array. If the element did not represent a glucose unit, a new element was chosen randomly until a glucose unit was selected. We assumed that this glucose unit was bound to the subsite at the right of the location of hydrolysis. In other words, the bond toward the non-reducing end might be hydrolyzed. If there was no bond, because the glucose unit selected is a non-reducing end, this attack was called non-productive. If the bond was situated next to an α-1,6-linked glucose unit, we assumed that it could not be hydrolyzed (French et al., 1972) and was therefore also non-productive. The bonds in maltose and maltotriose could also not be hydrolyzed

(Kandra et al., 2002; Marchal et al., 1999; Saito, 1973). It was assumed that the substrate binding mode with the highest value for $k_{+2,r,n}K_{r,n}$ had a chance of hydrolysis of 1 (Marchal et al., 2003). If this binding mode was achieved with substrate size o and with the reducing end located at position p, the chance of hydrolysis was defined as follows:

$$p_{r,n} = \frac{k_{+2,r,n}K_{r,n}}{k_{+2,p,o}K_{p,o}} \tag{4}$$

Note that the denominator is constant, while the numerator varies depending on substrate size and binding mode.

Besides a difference in affinity and hydrolysis rate, the influence of branch points (α-1,6-linkages) was also taken into account as described by Marchal et al. (2003). They distinguished three types of inhibition due to α-1,6-linkages. Inhibition type I is assumed to affect the enzyme during hydrolysis of α-1,4-linkages near a branch-starting glucose unit. In Figure 1, inhibition type I takes place in chains 2 and 3 close to glucose units labeled with index 4. In the vicinity of side branches, enzyme inhibition also takes place either toward the reducing end (type II) or toward the non-reducing end (type III; see Fig. 1). Inhibition was taken into account when an α-1,6-linkage is less than 5 glucose units apart from the location of hydrolysis (Marchal et al., 2003). For the amylopectin molecule shown in Figure 1, at least one type of inhibition holds for each glucose unit. Each type of inhibition is described using an inhibition factor, $k_{\text{br\_in}}$, which is defined as follows:

$$k_{\text{br\_in}} = 2 - \exp(b_T y) \tag{5}$$

where b_T is the inhibition constant for the type of inhibition and y the number of glucose units between the location of hydrolysis and the α-1,6-linked glucose unit. When $k_{\text{br\_in}}$ was smaller than 0, it was considered to be 0. The chance on hydrolysis $p_{r,n}$ was multiplied by $(1 - k_{\text{br\_in}})$ for each type of inhibition. For more details on the inhibition by α-1,6-linked glucose units, we refer to Marchal et al. (2003).

To determine whether hydrolysis would take place, a random number between 0 and 1 was generated; if it was smaller than the chance of hydrolysis, the attack was productive and the bond was hydrolyzed. This involved changing the glucose unit at subsite position +1 of the subsite map into a non-reducing end (unless a single glucose was split off) and converting the unit at subsite position −1 to a reducing end. The time was increased with t_p for a productive attack and t_{np} for a non-productive attack (Wojciechowski et al., 2001).

The simulations were ended after a pre-defined model time of hydrolysis. At set intervals (to save disk space and calculation time), the content of the substrate matrix was analyzed to determine the saccharide composition and DE. The DE was calculated with

$$\text{DE} = \frac{180.16 \times n_{re}}{162.14 \times n_{gl} + 18.02 \times n_{re}} \times 100 \tag{6}$$

where n_{re} stands for the number of reducing ends and n_{gl} stands for the number of glucose units in the substrate matrix (Marchal et al., 2003). Carbohydrates with a DP up to 7 (both branched and linear) were counted each time interval, because these carbohydrates could be measured with our HPLC system. If desired, all carbohydrates could be taken into account by the model, but this would require much more calculation time and disk space and this was therefore not attempted.

Although the effect of temperature was not considered in this article, it can be taken into account by this model as all equations that have been used to take into account the affinity of the enzyme for different substrates are temperature dependent (Eqs. 2 and 3 and therefore also Eq. 4). Enzyme deactivation, which is greatly affected by temperature, can be taken into account by increasing the time required for productive and non-productive attack according to the relevant deactivations mechanism. In the case of first order enzyme deactivation, the enzyme activity can be calculated as function of time if the deactivation constant k is known and with this information, the duration of each time step can be determined with the following equation:

$$\Delta t_{l+1} = \Delta t_l \frac{A_{l-1}}{A_l} \tag{7}$$

Where Δt_{l+1} is the time required for a productive or non-productive attack (it is either equal to t_p or t_{np}) after the previous time step Δt_l, A_{l-1} is the enzyme activity at the start of the previous time step and A_l is the enzyme activity at the end of Δt_l. The use of Eq. (7) can be illustrated by considering the first two time steps. Assuming that the first time step was productive, the second time step Δt_{l+1} is equal to

$$\Delta t_2 = \Delta t_1 \frac{A_0}{A_1} = t_p \frac{A_0}{A_0[\exp(-kt_p)]} = \frac{t_p}{\exp(-kt_p)} \tag{8}$$

This procedure can be repeated for the following time steps to take into account enzyme deactivation.

Materials and Methods

Materials

Wheat starch (S5127) was obtained from Sigma–Aldrich (Steinheim, Germany) and it had a moisture content of 9.95 ± 0.43 w/w% (based on 22 measurements, 95% confidence interval). The moisture content was determined by drying the wheat starch in a hot air oven at 105°C or in a vacuum oven at 80°C until the mass of the samples was constant in time. The water content of wheat starch was taken into account during all experiments. Thermostable α-amylase from *B. licheniformis* (EC 3.2.1.1, Termamyl 120L, type XII-A) was obtained from Sigma–Aldrich Chemie B.V. (Zwijndrecht, The Netherlands) and

α-amylase from *B. amyloliquefaciens* (BAN 480L) was donated by Novozymes (Bagsværd, Denmark). The enzyme concentration used during the experiments is expressed in mass percent of this enzyme stock solution per equivalent dry mass of substrate (w/w%). Fuming hydrochloric acid, sodium hydroxide, sodium chloride, calcium chloride dihydrate, calcium chloride, and trisodium phosphate were bought from Merck (Darmstadt, Germany). Maleic acid (disodium salt) was obtained from Acros Organics (Geel, Belgium). Maltohexaose from Serva was obtained from Brunschwig Chemie BV (Amsterdam, the Netherlands). All chemicals were at least analytical grade. Milli-Q water was used for all experiments.

Microcon YM-30 centrifuge filters (Millipore Corporation, Bedford, MA) were used to remove the enzyme from the hydrolyzate. Before the actual filtration, these filters were washed by centrifugation with 500 μL Milli-Q water during 40 min at 25°C and 13,000*g*.

Methods

Experimental Set-up and Sampling

For the validation of the model, hydrolysis experiments were carried out in a temperature-controlled batch reactor (liquid volume 200 mL) equipped with an anchor stirrer. Prior to enzymatic hydrolysis, the 10 w/w% wheat starch–water mixture containing 5.0 mM $CaCl_2$ was heated to approximately 90°C and was kept at this temperature for 1 h to ensure complete starch gelatinization. After the gelatinization treatment, the reactor content was cooled to 50°C. When the temperature inside the reactor was 50 ± 1°C, enzyme was added to the reactor (starting point of the hydrolysis reaction). The hydrolysis temperature in the reactor was kept at 50 ± 1°C during hydrolysis experiments. The stirrer speed during gelatinization and hydrolysis was equal to 300 rpm.

Hydrolysis of maltohexaose was carried out in a 1.5 mL safe-lock tube (Eppendorf AG, Hamburg, Germany). First, the reaction mixture excluding maltohexaose was heated to 50°C. After this temperature was reached, maltohexaose was added to obtain a 10 w/w% maltohexaose–water mixture (starting point of the hydrolysis reaction). Hydrolyis was carried out at 50 ± 1°C.

Samples were taken during the course of the experiments to determine the carbohydrate composition and the residual α-amylase activity. Due to the small sample volumes used during the maltohexaose hydrolysis experiment, the sample was first diluted to obtain a carbohydrate concentration of 10 g L^{-1} and a NaOH concentration of 0.1 M (for analysis of the carbohydrate composition) or to obtain an enzyme concentration of 20 mg L^{-1} (for enzyme activity measurements). All samples were frozen in liquid nitrogen to stop the hydrolysis reaction. The sample was kept in liquid nitrogen for at least 15 min and afterwards it was stored in a −80°C freezer.

The samples that were taken during the experiment with maltohexaose could be used for analysis directly after defrosting. The samples taken during the other experiments had to be diluted first. These frozen samples were grinded in a mortar with a pestle while submerging the sample in liquid nitrogen. The remainder of the sample preparation procedure used before analysis is reported elsewhere together with the procedures followed to determine the carbohydrate composition and the α-amylase activity (Baks et al., 2007). The DE was calculated from the weight fractions of glucose to maltohexaose using the method developed by Kiser and Hagy (1979) and adapted by Baks et al. (2007).

The carbohydrate composition measurements were used to determine the weight fraction of a specific carbohydrate with the following equation:

$$X_{w,i} = \frac{C_{DPi}}{C_{tot} + M_{w,w} \cdot (\sum_{j=1}^{7} C_{m,DPj})} \quad (9)$$

where C_{DPi} (g L^{-1}) is the mass-based concentration of a carbohydrate with DP *i*, $C_{m,DPj}$ (mol L^{-1}) the mole-based concentration of a carbohydrate with DP *j*, C_{tot} is total carbohydrate concentration (g L^{-1}), and $M_{w,w}$ the molar mass of water (18 g mol^{-1}). The total carbohydrate concentration was corrected for the increase in dry matter during the reaction caused by the formation of maltooligosaccharides smaller than maltooctaose. In case maltohexaose was used as a substrate, all reaction products can be quantified and Eq. (10) was used to calculate the oligosaccharide weight fraction

$$X_{w,i} = \frac{C_{DPi}}{(\sum_{j=1}^{6} C_{DPj})} \quad (10)$$

where C_{DPj} (g L^{-1}) is the mass-based concentration of a carbohydrate with DP *j*.

Model Simulations

For each simulated starch hydrolysis process, a new starch substrate was built up with approximately 100,000 glucose units in total. For the modeling of amylopectin the chain length distribution as reported in Table II of Hizukuri and Maehara (1990) was used. For amylose, the distribution shown in Figure 4 of Hanashiro and Takeda (1998) was incorporated.

For the simulated hydrolysis of the substrate, the subsite map for BLA determined by Kandra et al. (2002) and the subsite map for BAA obtained by Allen and Thoma (1976b) were used (see Table I). For both α-amylases, we used 0.1, 0.2, and 0.4 for respectively inhibition constants b_I, b_{II}, and b_{III} (Marchal et al., 2003).

The results obtained with the simulations were compared to the experimental data to obtain values for t_p and t_{np}, by comparing initial rates of hydrolysis. Model simulations were performed three times and averaged (except for the

Table I. Subsite maps with the apparent binding energy per subsite (kJ mol^{-1}) used for the model simulations from Kandra et al. (2002) for BLA, and from Allen and Thoma (1976b) for BAA.

Subsite	−6	−5	−4	−3	−2	−1	+1	+2	+3	+4
BLA	0	−11.1	−2.7	−5.1	−6.5	0	0	−5.1	−5.8[b]	8
BAA[a]	−4.48	−10.21	−0.67	−4.23	−9.54	13.81	−14.39	−7.2	−4.02	5.27

The location of hydrolysis is in between subsites −1 and +1, and the glucose unit with the reducing end must be located such that it is the outmost right glucose unit.

[a]Including the acceleration factor, ΔG_a.

[b]For the modified subsite map of BLA, the binding energy of subsite +3 was set to 0 kJ mol^{-1}.

modified subsite map of BLA, which was performed only once), neglecting small differences in the time intervals between the different simulations. For each individual simulation, the model time was then converted to actual reaction time by non-linear fitting of the modeled DE (in case the hydrolysis of starch was simulated) or maltohexaose weight fraction (in case maltohexaose hydrolysis was simulated) to the corresponding experimental values. The modeled data in the linear part of the curve were fitted to experimental data in the corresponding region. In case of maltohexaose, the first 6 h of hydrolysis were used for the fitting procedure. We used a ratio t_p:t_{np} of 20:7, which was also used by Wojciechowski et al. (2001).

Matlab 7.0.1 (The MathWorks, Inc., Nattick, MA) was used to perform the model simulations. The Matlab standard random number generator was changed to another state for each simulation.

Results

The manner in which the subsite mapping theory was applied in this article was similar to the approach of Marchal et al. (2003). However, we used a simpler, more efficient matrix representation of the substrate. Comparison of their results with ours (on the saccharide composition as function of the DE) showed that our model yielded comparable results. Time (not considered in the model by Marchal et al.) was incorporated in our model with use of the theory of productive and non-productive attack developed by Wojciechowski et al. (2001). In case enzyme deactivation would take place, the times required for productive and non-productive attack would increase. Enzyme activity measurements in time showed that enzyme deactivation was negligible at our reaction conditions (results not shown) and therefore enzyme deactivation was not taken into account.

Linear and branched carbohydrates with the same molecular weight cannot be separated with the HPLC column that was used for carbohydrate analysis. However, our stochastic model can discriminate between linear and branched carbohydrates. For hexasaccharides and heptasaccharides, the predicted weight fractions of both the linear carbohydrates and the total amount of carbohydrates (branched and linear) are shown. In principle, branched pentasaccharides are also formed, but their weight fractions were so low that they are not shown.

Enzymatic Starch Hydrolysis by BLA

Figure 2 shows the predicted and experimental results of the hydrolysis of wheat starch by BLA. Figure 2A shows that both the simulated and the experimentally obtained DE rapidly increased during the first stage of hydrolysis. However, this linear stage took about 120 min for the experimental data and 60 min for the simulated data. After this stage a more gradual increase of the DE was observed. The predicted DE was underestimated as compared to the experimental data.

In case of carbohydrates ranging from glucose to pentasaccharide, both the experimental and simulated weight fractions increased over the complete time course. Both the weight fractions of hexa- and heptasaccharide reached a maximum before they gradually started to decrease. Although the simulated data for BLA showed the same trends and order of magnitude as the experimental data, the absolute weight fractions of glucose, maltose (Fig. 2B), maltotetraose, and pentasaccharide (Fig. 2C) were underestimated by the model. The predicted weight fraction of maltotriose was higher than the weight fraction that was determined experimentally (Fig. 2B). The observed maximum in the weight fraction versus time curves of hexasaccharide and heptasaccharide were correctly predicted by our model (Fig. 2D). In case of hexasaccharide, however, a lower maximum value was predicted compared to the value that was found experimentally. In addition, the simulated weight fractions of hexasaccharide and heptasaccharide decreased less rapidly after the maximum had been reached in comparison with the experimental data. Based on the model, it seems that the contribution of branched carbohydrates to the total amount of hexasaccharide and heptasaccharide is significant.

Enzymatic Starch Hydrolysis by BAA

Figure 3 shows the DE and weight fractions of several small carbohydrates based on experimental and simulated data for the hydrolysis of wheat starch by BAA. Both the experiment and the model predictions showed a DE that rapidly increased during the first half hour followed by a more gradual increase afterwards (Fig. 3A). In general, the agreement between simulation and experiments is much better than with BLA, although the predicted DE was somewhat lower than the experimental DE when the time of hydrolysis exceeded 1 h.

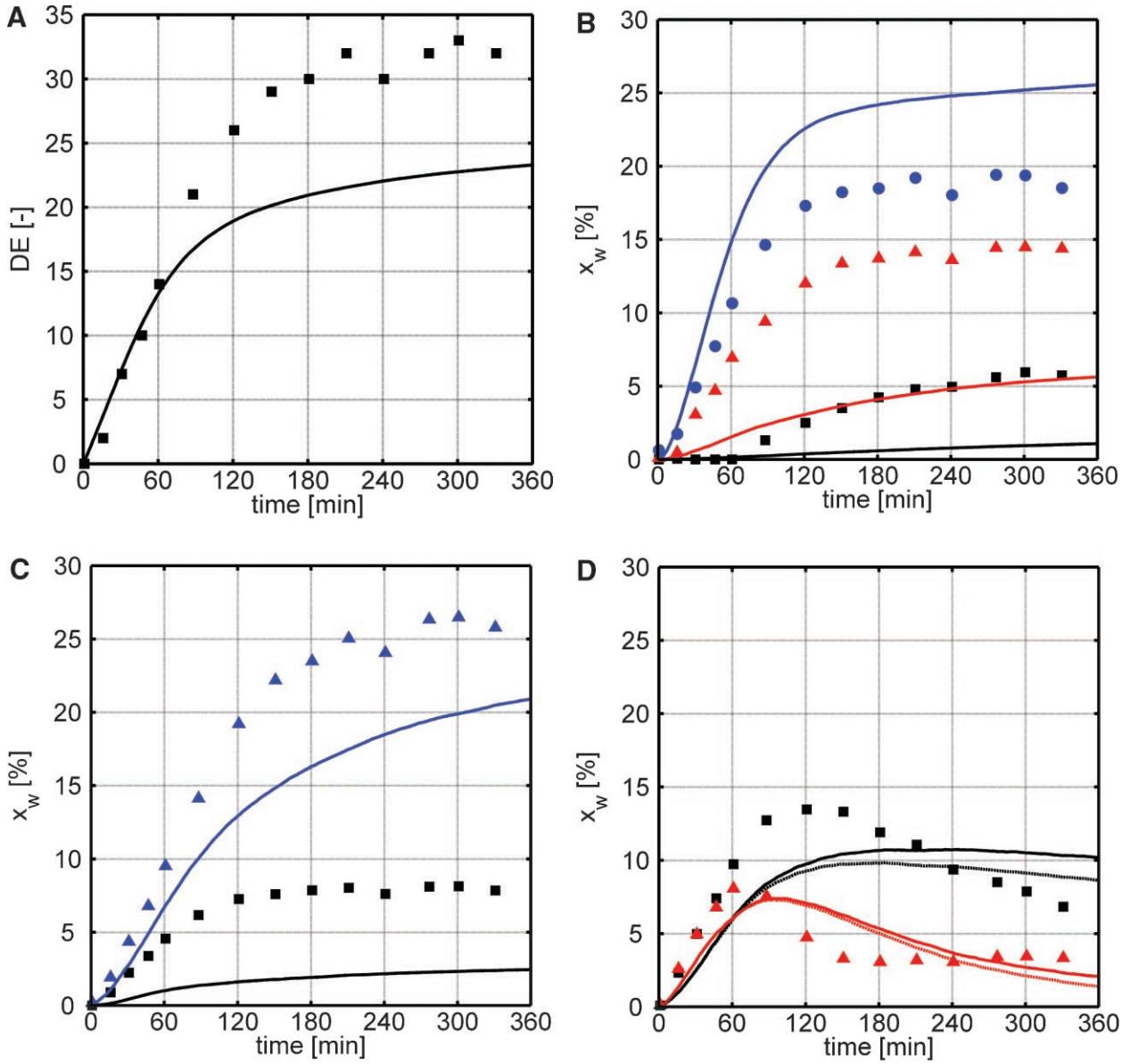

Figure 2. Experimental and predicted data obtained during enzymatic hydrolysis of 5 w/w % wheat starch with 0.01 w/w % BLA at 50°C. **A:** contains the experimental (■) versus simulated (solid line) dextrose equivalent; **B:** contains the experimental weight fractions of glucose (■), maltose (▲) and maltotriose (●) versus simulated (respectively black, red, and blue solid line) weight fractions; **C:** contains the experimental weight fractions of maltotetraose (■) and total pentasaccharide (▲) versus simulated weight fractions (respectively black and blue solid line); **D:** contains the experimental weight fractions of hexasaccharide (■) and heptasaccharide (▲) versus simulated linear and total hexasaccharide (respectively black dashed and solid line) and linear and total heptasaccharide (respectively red dashed and solid line) weight fractions.

In Figure 3B–D, the simulated results show that the same trend and order of magnitude are found as observed during the experiment. However, the weight fractions of glucose, maltose (Fig. 3B), and maltotetraose (Fig. 3C) were underestimated by the model, while the maltotriose and pentasaccharide weight fractions were overestimated. The predicted weight fraction of hexa- and heptasaccharide, however, agreed well with the experimental values. Similar as observed during the simulations with BLA, we found that the contribution of branched carbohydrates to the total amount of hexasaccharide and heptasaccharide is significant.

Enzymatic Maltohexaose Hydrolysis by BAA

Enzymatic hydrolysis of maltohexaose with BAA resulted in a continuous increase in the weight fractions of all smaller carbohydrates during the complete time course of the experiment (Fig. 4). The model predictions showed the

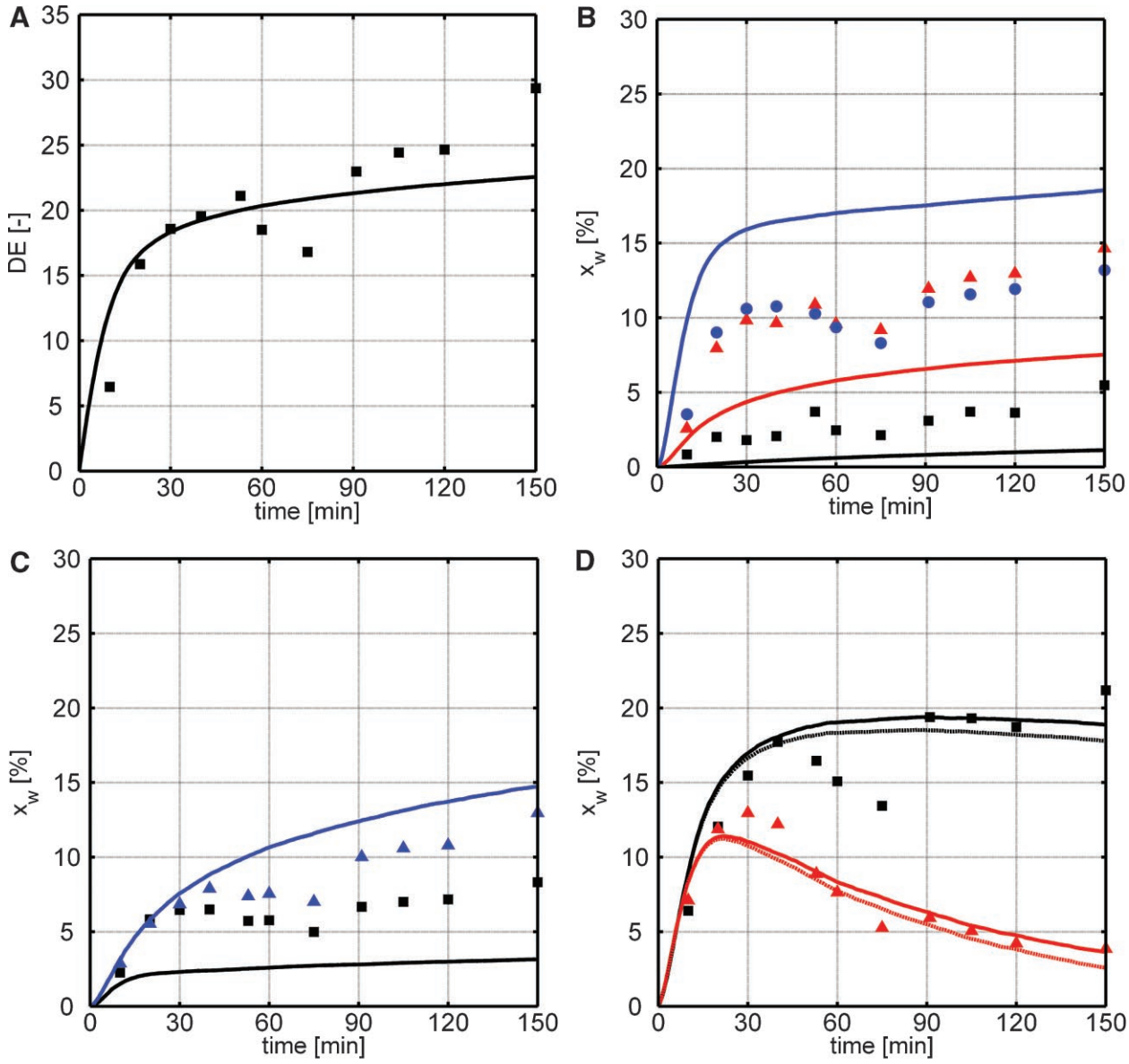

Figure 3. Experimental and predicted data obtained during enzymatic hydrolysis of 5 w/w % wheat starch with 0.01 w/w % BAA at 50°C. Legend: see Figure 2.

same trend and the correct order of magnitude of the predicted weight fraction. However, the weight fraction of maltotriose was overestimated while the weight fraction of maltose and maltotetraose were underestimated. The predictions of the glucose, maltopentaose, and maltohexaose weight fractions were comparable to the corresponding experimental values.

Effect of BLA Subsite Map on Enzymatic Starch Hydrolysis

According to the experimental data in Figure 2B, maltose and maltotriose were formed in approximately the same amounts when wheat starch is hydrolyzed by BLA. As a result, one expects a negligible difference between the energy of binding of two or three glucose units at the left or right of the location of hydrolysis in the subsite map. The BLA subsite map obtained by Kandra et al. (2002) (Table I) showed a clear preference for splitting off maltotriose from the reducing end as compared to maltose and other saccharides, because occupation of subsite +3 with binding energy -5.8 kJ mol^{-1} results in a much lower total energy of binding. We therefore evaluated whether a better fit for maltose and maltotriose would be obtained when the binding energy of subsite +3 in the subsite map for BLA is set to 0 kJ mol^{-1}. After modification of the subsite map, the DE agreed better with the experimental values (Fig. 2A vs. Fig. 5A) due to the increased glucose and maltose weight fraction (Fig. 2B vs. Fig. 5B). The simulated weight fractions

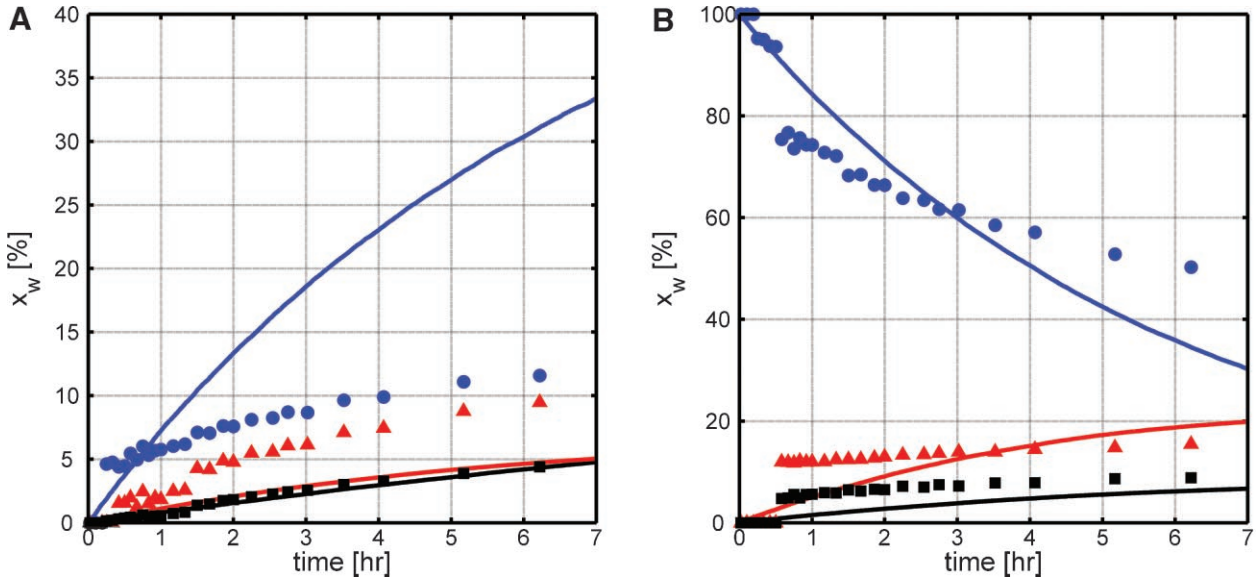

Figure 4. Experimental and predicted data obtained during enzymatic hydrolysis of 10 w/w % maltohexaose with 0.01 w/w % BAA at 50°C. **A:** contains the experimental weight fractions of glucose (■), maltose (▲) and maltotriose (●) versus simulated (respectively black, red, and blue solid line) weight fractions; **B:** contains the experimental weight fractions of maltotetraose (■), maltopentaose (▲), and maltohexaose (●) versus simulated weight fractions (respectively black, red, and blue solid line).

glucose, maltose, maltotriose (Fig. 5B), and pentasaccharide (Fig. 5C) showed a reasonable agreement with experimental data after changing the subsite map. However, the modified subsite map did not lead to an improvement for maltotetraose (Fig. 5C) and hexasaccharide and heptasaccharide (Fig. 5D). These results were confirmed by the squared sum of differences between experimental and simulated data for the two subsite maps as shown in Table II. Note that the differences for maltotetraose, total hexasaccharide and total heptasaccharide were larger with the modified subsite map than with the original subsite map.

Effect of t_p:t_{np} Ratio on Enzymatic Starch Hydrolysis by BAA

The predictions shown in the previous figures were obtained with a fixed t_p:t_{np} ratio of 20:7 based on the article of Wojciechowski et al. (2001). Figure 6 shows the results of a fit in which the t_p:t_{np} ratio was changed to 66:1. Changing the t_p:t_{np} ratio improved the fit between the experimental and modeled DE (Fig. 6A). The predicted weight fractions of glucose, maltose (Fig. 6B), and maltotetraose (Fig. 6C) agreed better with the experimental data as compared to the predictions shown in Figure 3. However, the weight fractions of maltotriose (Fig. 6B), pentasaccharide (Fig. 6C), hexasaccharide and heptasaccharide (Fig. 6D) deviated more from the experimental data compared to the predicted values obtained with the old t_p:t_{np} ratio. The squared sums of differences between the experimental and simulated data for both fits are shown in Table II. Based upon these values, it is difficult to decide which t_p:t_{np} ratio leads to the best predictions.

Discussion

Although the predicted weight fractions of carbohydrates with a DP up to 7 were of the same order of magnitude as the experimentally determined weight fractions and they also showed the same trend, the absolute values were not predicted correctly. The same holds for the DE as function of time. Wojciechowski et al. (2001) compared the model output with the experimental values based on the reducing power of the reaction mixture, which is comparable to the DE. The differences between the model and experimental data of Wojciechowski et al. are smaller than the differences that we have observed. However, reducing power or DE measurements are not suitable for the purpose of defining the product, because the same DE can be found for products with a different carbohydrate composition. One should therefore also compare the model output and the experimental values based upon the concentrations of the carbohydrates. The model output of Marchal et al. (2003) is comparable to our model output. However, with our model it is possible to describe the formation and break down of all carbohydrates during enzymatic hydrolysis in time. Deviations of the model data from the experimental data can be a result of several factors. The main factors that might cause these deviations are the substrate model, the subsite map, the hydrolysis behaviour of the α-amylase and the time scale.

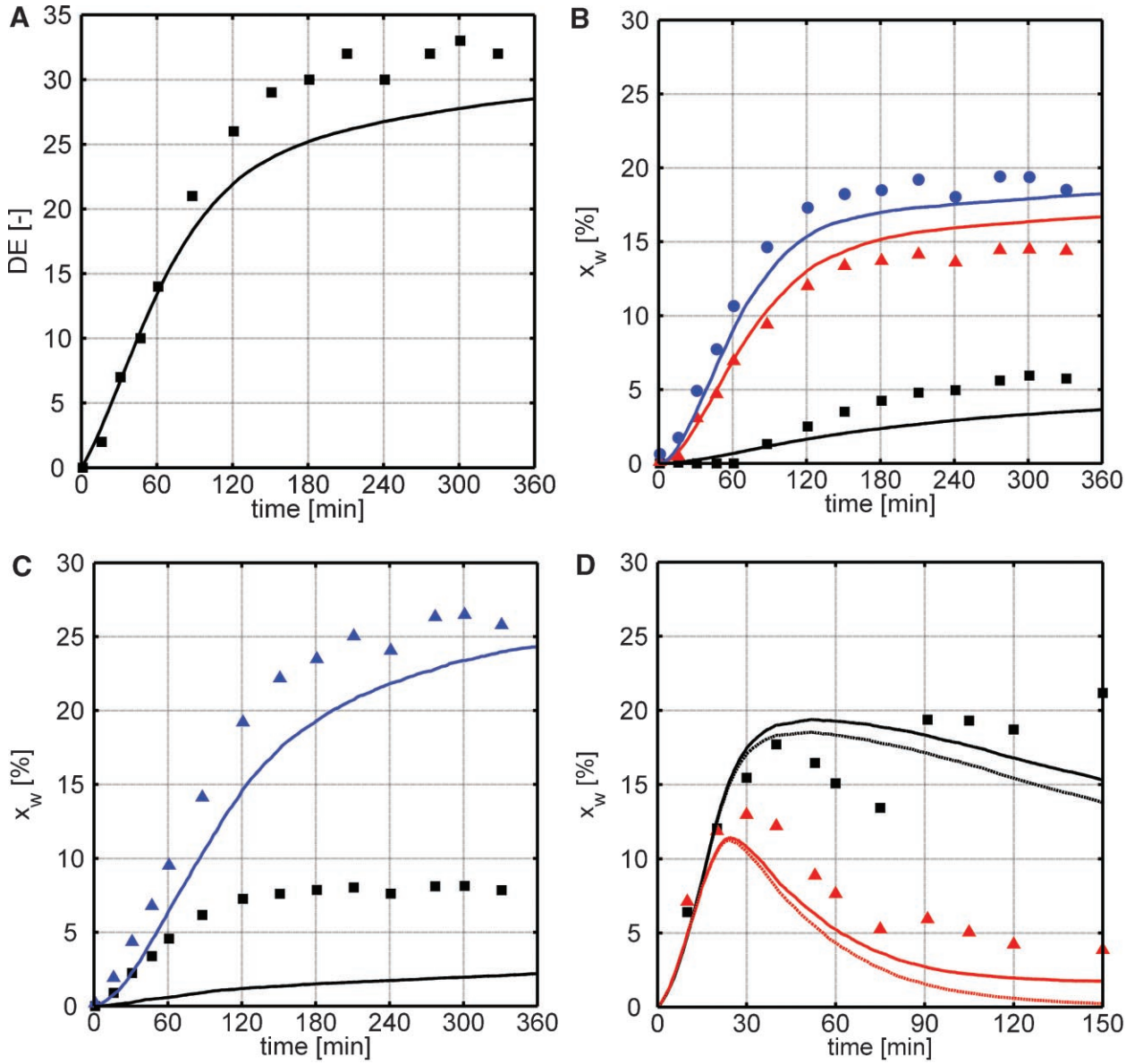

Figure 5. Experimental and predicted data (based on 1 simulation) obtained during enzymatic hydrolysis of 5 w/w % wheat starch with 0.01 w/w % BLA at 50°C. For the simulated data, subsite +3 of the subsite map determined by Kandra et al. (2002) was set to 0 (see Table 1). Legend: see Figure 2.

Table II. Squared sum of differences between experimental data points and corresponding model data (Figs. 2–6) before and after changing the subsite map (BLA1 vs. BLA2; see Table I), before and after changing t_p:t_{np} (BAA1 = 20:7 and BAA2 = 66:1), and for hydrolysis of maltohexaose (BAA3, standard conditions).

	DE[a]	DP1[b]	DP2[b]	DP3[b]	DP4[b]	DP5[b]	DP6[b]	DP7[b]
BLA1	666.9	131.7	787.1	339.4	310.0	382.5	96.4	34.2
BLA2	174.1	33.5	24.7	28.2	358.8	144.2	218.1	116.2
BAA1	119.1	63.0	272.7	459.5	149.3	63.3	76.5	14.5
BAA2	70.5	46.6	192.4	589.8	127.6	252.2	107.4	68.4
BAA3	—	3.0	207.0	1,371.3	287.0	593.5	1,769.6	—

[a]Dextrose equivalent.
[b]DP1, . . ., DP7 stand for glucose, maltose, maltriose, maltotetraose, pentasaccharide, hexasaccharide, and heptasaccharide.

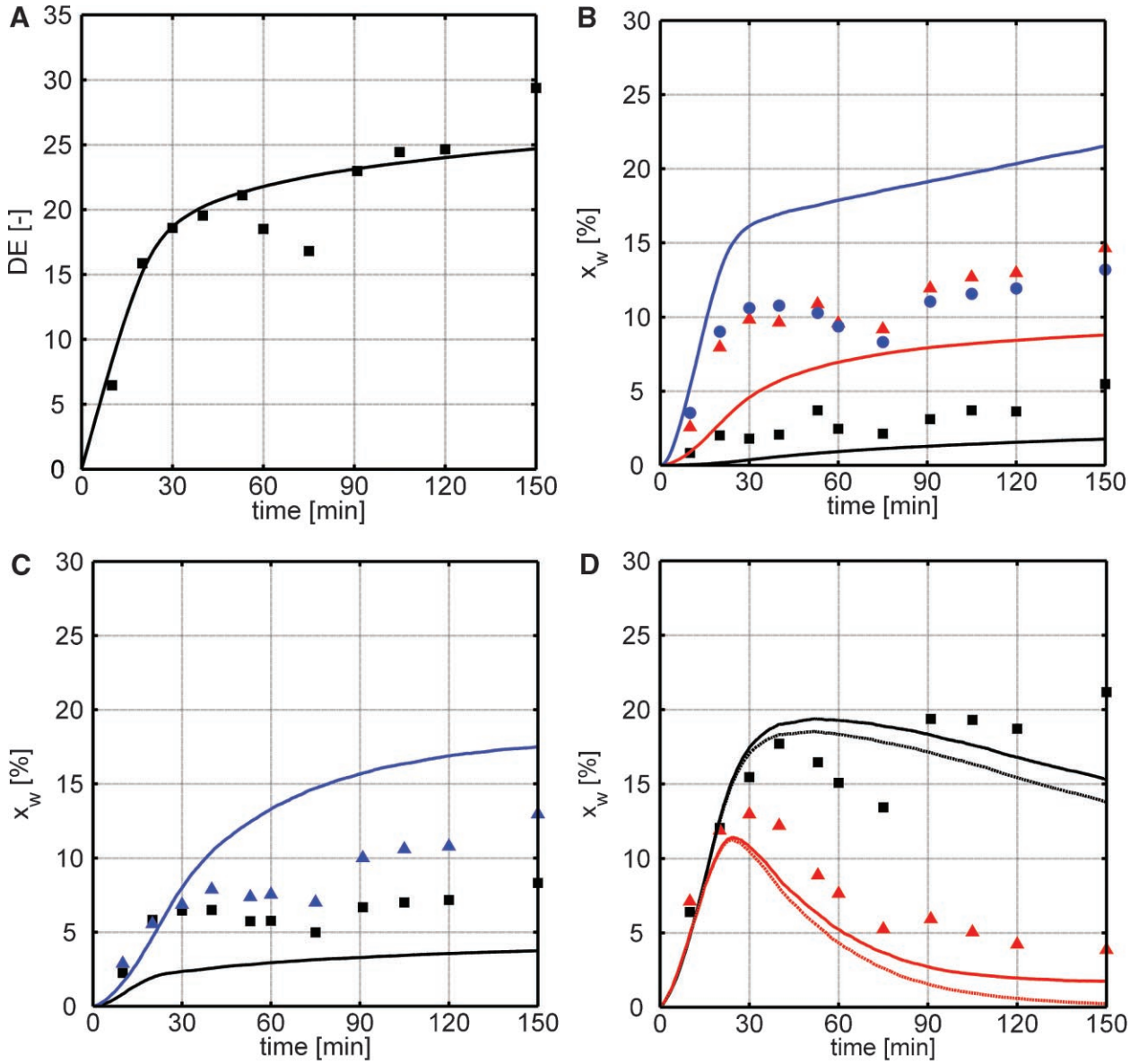

Figure 6. Experimental and predicted data obtained during enzymatic hydrolysis of 5 w/w % wheat starch with 0.01 w/w % BAA at 50°C. The t_p:t_{np} ratio was changed from 20:7 to 66:1. Legend: see Figure 2.

Substrate Model

The input for our amylopectin model was based on the chain length distribution of amylopectin in wheat starch and the model randomly inserted branch points. The model of Marchal et al. (2001) used a more structured distribution of branch points, which agrees better with the real structure of amylopectin. Use of our substrate model or use of the substrate model developed by Marchal et al. (2001) in our hydrolysis model resulted in approximately the same differences between the experiments and the model predictions. In case maltohexaose was used as a substrate, which is well defined and easy to model, the predicted values were still not comparable with the experimental values for all carbohydrates that were considered. Consequently, it seems that the substrate model did not cause the deviations between experimental and predicted weight fractions.

Subsite Map

Another reason for the deviation between the predicted results and the experimental results can be caused by the subsite map that was used as these subsite maps might be affected by the type of substrate used to determine them. Torgerson et al. (1979) and Allen and Thoma (1976b) used

radioactive oligosaccharides to determine the subsite maps of BAA. These radioactive oligosaccharides were assumed to be chemically similar to normal saccharides. Kandra et al. (2002) used 2-chloro-4-nitrophenyl (CNP) β-glycosides ranging from maltotetraose to maltodecaose to determine the subsite map of BLA. They mentioned that the CNP group can also interact with subsites +2 and +3, which might lead to deviations for the subsite map obtained using radioactive or normal oligosaccharides. Unfortunately, it has not been investigated whether different types of substrates would result in different subsite maps and different model predictions. In addition, the subsite maps were used in our model to predict the hydrolysis of a wide range of carbohydrates including large carbohydrates, while only small carbohydrates were used to determine these subsite maps.

The experimental results (Figs. 2–6) indicate that maltose and maltotriose are formed in comparable amounts. Paolucci-Jeanjean et al. (2000) found similar results when cassava starch is hydrolyzed by BLA at a higher temperature. However, the subsite map for BLA (Kandra et al., 2002) clearly indicates the enzyme's preference to split off maltotriose from the reducing end; the lowest energy of binding at the right side of the location of hydrolysis can be obtained when subsites +1, +2, and +3 are filled. By setting the subsite energy of subsite +3 to 0, the influence of this subsite was illustrated. After this modification, the predicted weight fractions of maltose and maltotriose were comparable (Fig. 5), leading to a better description of the experimental data for maltose and maltotriose (see Table II). To better fit the model data to the experimental data, a new subsite map could be obtained by fitting the model predictions to the experimental hydrolysis results. However, the validity of this approach is questionable given the large number of fit parameters that would be involved, and since our aim was to compose a model with a limited amount of independent experimental input, we did not consider this route.

Hydrolysis Behaviour of α-Amylase

Besides the hydrolysis behavior of α-amylase incorporated in the subsite map, other specific hydrolysis phenomena may take place that were not taken into account in our model. For example, it is known that some α-amylases exhibit a repetitive-attack mechanism, which could give rise to higher amounts of maltose and glucose (MacGregor and MacGregor, 1985). This would also result in a higher DE. Furthermore, it is possible that carbohydrates form a non-productive complex with the enzyme without blocking the catalytic site and the subsites surrounding it. This resulting enzyme–carbohydrate complex might still be active, because in some cases it can still hydrolyze another substrate even at higher hydrolysis rates (Baks et al., 2006). Once more, the predicted DE might increase leading to a better agreement between predicted and experimental values.

Finally, by having a purely random selection of an α-1,4-linkage for hydrolysis, it was assumed that the chance that an enzyme will attack an oligosaccharide is proportional to the number of glucose monomers it contains, and that all parts of the molecule are equally accessible to the enzyme. However, it might be possible that the volume occupied by branched and linear carbohydrates with the same degree of polymerization differs, which might affect the chance that α-amylase encounters such a substrate. It should therefore be determined whether it is fair to assume that the chance of enzymatic hydrolysis of an oligosaccharide is proportional to the degree of polymerization. It is unclear how such changes will affect the outcome of the model.

Time Scale

For the model presented in this article, the t_p:t_{np} ratio of 20:7 was used that was proposed by Wojciechowski et al. (2001), but they did not mention how they determined this ratio. Since the BAA subsite map seemed to be more reliable than the BLA subsite map, it was decided to illustrate the effect of a different t_p:t_{np} ratio for the hydrolysis predictions with BAA. Changing this ratio indeed affected the outcome of the simulations and it should therefore be investigated whether the t_p:t_{np} ratio can be determined independently instead of using a fit procedure to obtain this ratio. Molecular modeling might be used to determine the theoretical t_p:t_{np} ratio that is expected for various substrates with α-amylase. In addition, this ratio might also differ for different carbohydrates, because of variations in intra- and intermolecular mobility into and out of the enzyme's active site.

During wheat starch hydrolysis experiments, enzyme activity measurements indicated that the enzyme was stable at our reaction conditions. However, it is possible to include changes in the enzyme activity during hydrolysis. In case enzyme deactivation would take place, the actual values of t_p and t_{np} can be increased in time. The activity of BLA was studied quite extensively (De Cordt et al., 1992, 1994; DeClerck et al., 1997; Dobreva et al., 1994; Fitter et al., 2001; Ivanova et al., 1993; Rodríguez et al., 2006b; Tomazic and Klibanov, 1988; Violet and Meunier, 1989) and these articles can be used as a starting point. Various conditions, such as temperature, calcium concentration, pH, enzyme concentration and substrate concentration, determine the initial enzyme activity as well as the decrease of this activity in time. Obtaining a general equation for the activity based on all the factors described in literature is not a trivial task. It is simpler and more accurate to determine the enzyme activity at the specific reaction conditions and subsequently implement this information in the t_p:t_{np} ratio used in the model.

Conclusions

The stochastic model presented in this article shows that it is possible to use the subsite theory to predict the saccharide

composition and DE in time for wheat starch hydrolysis with α-amylase. The relatively simple substrate model that was developed can be used as effective and efficient input for the hydrolysis model.

For both BAA and BLA, the predicted weight fractions and DEs showed the same trend as the corresponding experimental values. Although the order of magnitude of the predictions was comparable with the experimentally determined values, the absolute values calculated with the model differed from the experimental results. The model can therefore be used to gain insight in the dynamic formation and breakdown of all carbohydrates during enzymatic starch hydrolysis, but it is not yet suitable for absolute predictions of the oligosaccharide concentrations and DE. To improve the model predictions, it seems to be necessary to obtain a subsite map that can be used for longer hydrolysis times and larger carbohydrates. Such a subsite map may be obtained by fitting the model data to the experimental data. In addition, it may be useful to include the experimentally observed repetitive-attack mechanism for α-amylases in the model. Furthermore, a procedure should be developed to obtain a reliable ratio between the time required for the formation and break down of non-productive enzyme–substrate complexes and the time required for the formation of productive enzyme–substrate complexes and the subsequent release of the hydrolysis products. Research is also required to determine whether these reaction times depend on the carbohydrate chain length.

The model presented here was developed to describe the enzymatic hydrolysis of wheat starch by BAA and BLA, but it may well be converted to other depolymerase systems for which the subsite map is available. It is also be possible to include more than one enzyme in the model by the generation of an additional random number to select the enzyme that is going to interact with the substrate.

Nomenclature

A_i	enzyme activity at the end of time step i
BAA	α-amylase from *Bacillus amyloliquefaciens*
BLA	α-amylase from *Bacillus licheniformis*
b_T	inhibition constant
C_{DPi}	mass-based concentration of a carbohydrate with degree of polymerization i ($g\,L^{-1}$)
$C_{m,DPj}$	$C_{m,DPj}$ is the mole-based concentration of a carbohydrate with degree of polymerization j ($mol\,L^{-1}$)
C_{tot}	total carbohydrate concentration ($g\,L^{-1}$)
DE	dextrose equivalent
DP	degree of polymerization
E	enzyme
k	first order enzyme deactivation constant (s^{-1})
k_{+i}	pre-exponential factor for rate constant of reaction i
k_{br_in}	inhibition factor for hydrolysis near branching points in amylopectin
$k_{i,p,o}$	reaction rate constant of reaction i for carbohydrate with degree of polymerization p with the reducing end in position o leading to highest value of $k_{+2,r,n}K_{r,n}$ (s^{-1} for first order reactions and $m^3\,mol^{-1}\,s^{-1}$ for second order reactions)
$k_{i,r,n}$	reaction rate constant of reaction i for carbohydrate with degree of polymerization n when the reducing end is in position r (s^{-1} for first order reactions and $m^3\,mol^{-1}\,s^{-1}$ for second order reactions)
$K_{p,o}$	association constant for carbohydrate with degree of polymerization p with the reducing end in position o leading to highest value of $k_{+2,r,n}K_{r,n}$
$K_{r,n}$	association constant for enzyme with carbohydrate with degree of polymerization equal to n with the reducing end in position r
$M_{w,w}$	molar mass of water ($18\,g\,mol^{-1}$)
n_{gl}	number of glucose units
n_{re}	number of reducing ends
P_m	hydrolysis product with degree of polymerization m
P_{n-m}	hydrolysis product with degree of polymerization $n-m$
$p_{r,n}$	chance of hydrolysis when the reducing end of carbohydrate with degree of polymerization n is in position r
R	gas constant ($J\,mol^{-1}\,K^{-1}$)
S_n	substrate with degree of polymerization n
T	absolute temperature (K)
t_p	time required for a productive attack of the enzyme (s)
t_{np}	time required for non-productive attack of the enzyme (s)
x	number of occupied subsites
$x_{w,i}$	weight fraction of a carbohydrate with degree of polymerization i
y	number of glucose units between the location of hydrolysis and the α-1,6-linked glucose unit
ΔG_a	acceleration factor of the subsite map ($J\,mol^{-1}$)
ΔG_{mix}	entropic energy contribution for binding of two molecules ($J\,mol^{-1}$)
ΔG_i	binding energy of subsite i ($J\,mol^{-1}$)
Δt_l	Duration of time step in model for step l (s)

References

Allen JD, Thoma JA. 1976a. Subsite mapping of enzymes: Depolymerase computer modelling. Biochem J 159:105–120.

Allen JD, Thoma JA. 1976b. Subsite mapping of enzymes: Application of the depolymerase computer model to two α-amylases. Biochem J 159:121–132.

Baks T, Janssen AEM, Boom RM. 2006. A kinetic model to explain the maximum in α-amylase activity measurements in the presence of small carbohydrates. Biotechnol Bioeng 94:431–440.

Baks T, Kappen FHJ, Janssen AEM, Boom RM. 2007. Towards an optimal process for gelatinisation and enzymatic hydrolysis of highly concentrated starch-water mixtures. J Cereal Sci, in press. DOI: 10.1016/j.jcs.2007.03.011.

Brandam C, Meyer XM, Proth J, Strehaiano P, Pinguad H. 2003. An original kinetic model for the enzymatic hydrolysis of starch during mashing. Biochem Eng J 13:43–52.

Davies GJ, Wilson KS, Henrissat B. 1997. Nomenclature for sugar-binding subsites in glycosyl hydrolases. Biochem J 321:557–559.

De Cordt S, Vanhoof K, Hu J, Maesmans G, Hendrickx M, Tobback P. 1992. Thermostability of soluble and immobilized α-amylase from *Bacillus licheniformis*. Biotechnol Bioeng 40:396–402.

De Cordt S, Hendrickx M, Maesmans G, Tobback P. 1994. The influence of polyalcohols and carbohydrates on the thermostability of α-amylase. Biotechnol Bioeng 43:107–114.

Declerck N, Machius M, Chambert R, Wiegand G, Huber R, Gaillardin C. 1997. Hyperthermostable mutants of *Bacillus licheniformis* α-amylase: Thermodynamic studies and structural interpretation. Protein Eng 10:541–549.

Dobreva E, Ivanova V, Emanuilova E. 1994. Effect of temperature on some characteristics of the thermostable α-amylase from *Bacillus licheniformis*. World J Microbiol Biotechnol 10:547–550.

Ellis RP, Cochrane MP, Dale MFB, Duffus CM, Lynn A, Morrison IM, Prentice RDM, Swanston JS, Tiller SA. 1998. Starch production and industrial use. J Sci Food Agric 77:289–311.

Fitter J, Herrmann R, Dencher NA, Blume A, Hauss T. 2001. Activity and stability of a thermostable α-amylase compared to its mesophilic homologue: Mechanisms of thermal adaptation. Biochemistry 40: 10723–10731.

French D, Smith EE, Whelan WJ. 1972. The structural analysis and enzymatic synthesis of a pentasaccharide alpha-limit dextrin formed from amylopectin by *Bacillus subtilis* alpha-amylase. Carbohydr Res 22:123–134.

Hanashiro I, Takeda Y. 1998. Examination of number-average degree of polymerization and molar-based distribution of amylose by fluorescent labelling with 2-aminopyridine. Carbohydr Res 306:421–426.

Hizukuri S, Maehara Y. 1990. Fine structure of wheat amylopectin: The mode of A to B chain binding. Carbohydr Res 206:145–159.

Ivanova VN, Dobreva EP, Emanuilova EI. 1993. Purification and characterization of a thermostable alpha-amylase from Bacillus licheniformis. J Biotechnol 28:277–289.

Kandra L, Gyémánt G, Remenyik J, Hovánzski G, Lipták A. 2002. Action pattern and subsite mapping of Bacillus licheniformis α-amylase (BLA) with modified maltooligosaccharide substrates. FEBS Lett 518:79–82.

Kiser DL, Hagy RL. 1979. Estimation of dextrose equivalent value of starch hydrolysates from liquid chromatographic. In: Charalambous G, editor. Liquid chromatographic analysis of food and beverages, Vol. 2. New York: Academic Press, pp. 363–378.

Komolprasert V, Ofoly RY. 1991. Starch hydrolysis kinetics of *Bacillus licheniformis* α-amylase. J Chem Tech Biotechnol 51:209–223.

Kusunoki K, Kawakami K, Shiraishi F, Kato K, Kai M. 1982. A kinetic expression for hydrolysis of soluble starch by glucoamylase. Biotechnol Bioeng 24:347–354.

MacGregor EA, MacGregor AW. 1985. A model for the action of cereal alpha amylases on amylose. Carbohydr Res 142:223–236.

Marchal LM, van de Laar AMJ, Goetheer E, Schimmelpennink EB, Bergsma J, Beeftink HH, Tramper J. 1999. Effect of temperature on the saccharide composition obtained after α-amylolysis of starch. Biotechnol Bioeng 63:344–355.

Marchal LM, Zondervan J, Bergsma J, Beeftink HH, Tramper J. 2001. Monte Carlo simulation of the α-amylolysis of amylopectin potato starch. Part I: Modelling of the structure of amylopectin. Bioprocess Biosyst Eng 24:163–170.

Marchal LM, Ulijn RV, de Gooijer CD, Franke GTh, Tramper J. 2003. Monte Carlo simulation of the α-amylolysis of amylopectin potato starch. Part II: α-Amylolysis of amylopectin. Bioprocess Biosyst Eng 26:123–132.

Nakatani H. 1996. Monte Carlo simulation of multiple attack mechanism of α-amylase. Biopolymers 39:665–669.

Paolucci-Jeanjean D, Belleville MP, Zakhia N, Rios GM. 2000. Kinetics of cassava starch hydrolysis with Termamyl® enzyme. Biotechnol Bioeng 68:71–77.

Park JT, Rollings JE. 1994. Effects of substrate branching characteristics on kinetics of enzymatic depolymerization of mixed linear and branched polysaccharides: I. Amylose/amylopectin α-amylolysis. Biotechnol Bioeng 44:792–800.

Rodríguez VB, Alameda EJ, Gallegos JFM, Requena AR, López AIG. 2006a. Enzymatic hydrolysis of soluble starch with an α-amylase from *Bacillus licheniformis*. Biotechnol Prog 22:718–722.

Rodríguez VB, Alameda EJ, Gallegos JFM, Requena AR, López AIG. 2006b. Thermal deactivation of a commercial α-amylase from *Bacillus licheniformis* used in detergents. Biochem Eng J 27:299–304.

Rollings JE, Thompson RW. 1984. Kinetics of enzymatic starch liquefaction: Simulation of the high- molecular-weight product distribution. Biotechnol Bioeng 26:1475–1484.

Saito N. 1973. A thermophilic extracellular a-amylase from *Bacillus licheniformis*. Arch Biochem Biophys 155:290–298.

Thompson DB. 2000. On the non-random nature of amylopectin branching. Carbohydr Polym 43:223–239.

Tomazic SJ, Klibanov AM. 1988. Why is one *Bacillus* α-amylase more resistant against irreversible thermoinactivation than another? J Biol Chem 263:3092–3096.

Torgerson EM, Brewer LC, Thoma JA. 1979. Subsite mapping of enzymes. Use of subsite map to simulate complete time course of hydrolysis of a polymeric substrate. Arch Biochem Biophys 196: 13–22.

Violet M, Meunier JC. 1989. Kinetic study of the irreversible thermal denaturation of *Bacillus licheniformis* α-amylase. Biochem J 263:665–670.

Wojciechowski PM, Koziol A, Noworyta A. 2001. Iteration model of starch hydrolysis by amylolytic enzymes. Biotechnol Bioeng 75:530–539.